

## Electronic Supplementary Information

### **Core-shell structured hierarchically porous NiO microspheres with enhanced electrocatalytic activity for oxygen evolution reaction**

Yali Ma,<sup>a</sup> Xue Wang,<sup>a</sup> Xiaodong Sun,<sup>a</sup> Tunan Gao,<sup>a</sup> Yunling Liu,<sup>a</sup> Ling Zhang,<sup>b</sup> Qisheng Huo,<sup>a</sup> and Zhen-An Qiao\*<sup>a</sup>

<sup>a</sup> *State Key Laboratory of Inorganic Synthesis and Preparative Chemistry, College of Chemistry, International Joint Research Laboratory of Nano-Micro Architecture Chemistry (NMAC), Jilin University, Changchun 130012, P. R. China*

<sup>b</sup> *College of Chemistry, Jilin University, Changchun 130012, P. R. China*

\*E-mail:

qiaozhenan@jlu.edu.cn

**Characterization.** Scanning electron microscopy (SEM) images were obtained on a HITACHI SU8020 scanning electron microscopy with an accelerating voltage of 5 kV. Transmission electron microscopy (TEM) images were obtained on an FEI Tecnai G2 F20 S-Twin D573 field emission transmission electron microscope with an accelerating voltage of 200 kV. Powder X-ray diffraction (XRD) patterns were obtained using a Rigaku D/Max 2550 diffractometer with Cu K $\alpha$  radiation ( $\lambda = 1.5418 \text{ \AA}$ ) operated at 50 kV and 200 mA. Inductively coupled plasma (ICP) analyses were operated on a Perkin-Elmer Optima 3300DV ICP instrument. XPS was performed on an ESCALAB 250 X-ray photoelectron spectrometer with a monochromatic X-ray source (Al K $\alpha$   $h\nu = 1486.6 \text{ eV}$ ). N<sub>2</sub> adsorption-desorption isotherms were obtained at -196 °C on a Micromeritics ASAP 2420 surface area analyzer. Brunauer-Emmett-Teller (BET) surface areas were calculated from the linear part of the BET plot. Thermogravimetric analyses (TGA) were performed on a TA Q500 thermogravimetric analyzer with a heating rate of 10 °C min<sup>-1</sup> under a flow of air from 25 °C to 800 °C. The Fourier Transform Infrared Spectroscopy (FTIR) spectra were recorded on a Brüker IFS 66 V/S FTIR spectrometer with KBr pellets as the background. All electrochemical measurements were performed with a three-electrode system using a CH Instrument (Model 660E), in which the as-synthesized materials were used directly as the working electrode.

**Electrochemical Tests.** Electrocatalytic activities of the as-prepared catalysts for OER were evaluated on a CHI-660E electrochemical analyser. A three-electrode cell was employed using a glassy carbon electrode (3 mm in diameter) coated with nickel oxide products (the loading amount is about 1.4 mg cm<sup>-2</sup>) as working electrode, an Hg/HgO in NaOH (1 M) solution electrode as the reference electrode, and a Pt wire as the counter electrode. The OER experiments were carried out in 1 M KOH solution. The calibration of Hg/HgO reference electrode is performed in a standard three-electrode system with polished Pt wires as the working and counter electrodes, and the Hg/HgO electrode as the reference electrode. Electrolytes are pre-purged and saturated with high purity H<sub>2</sub>. Linear scanning voltammetry (LSV) is then run at a scanning rate of 1 mV s<sup>-1</sup>, and the potential at which the current crossed zero is taken to be the thermodynamic potential (*vs.* Hg/HgO) for the hydrogen electrode reactions. In 1 M KOH solution, the zero-current point is at -0.924 V, so E (RHE) = E (*vs.* Hg/HgO) + 0.924 V.

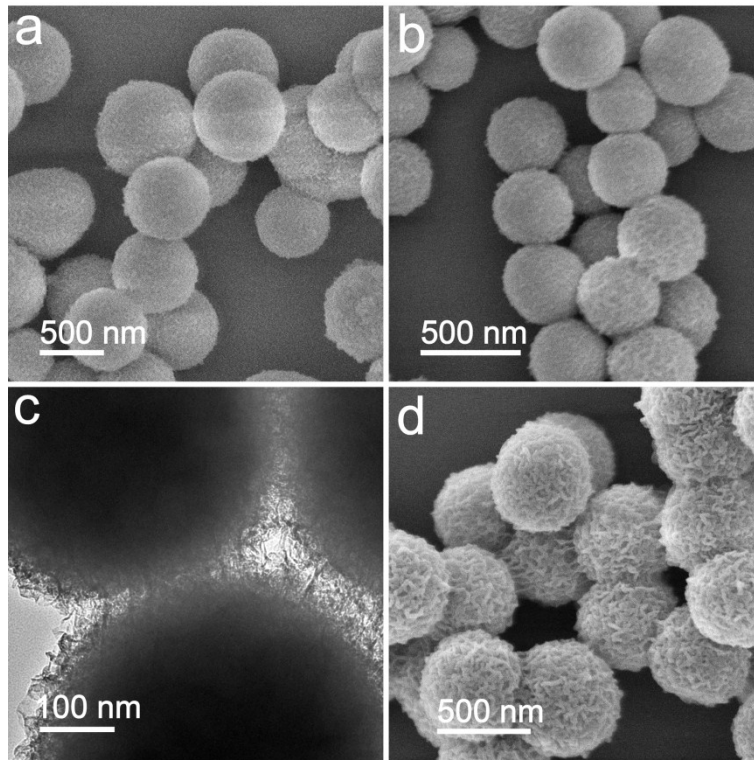


**Fig. S1** SEM and TEM images of the prepared hierarchical  $\text{Ni(OH)}_2$  microspheres synthesized at 85 °C with the HMTA/ $\text{Ni}^{2+}$  molar ratio of (a) 2; (b, c) 4; (d) 10.

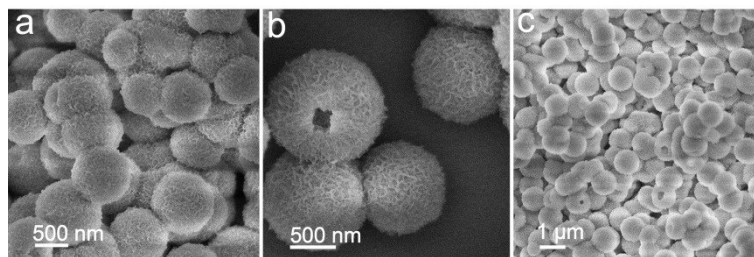


**Fig. S2** SEM images of the hierarchical  $\text{Ni(OH)}_2$  microspheres synthesized at 85 °C for (a) 24 h; (b) 48 h; (c) 84 h.

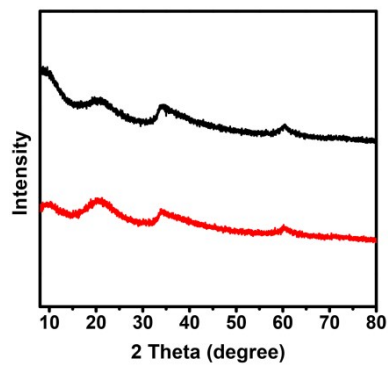


**Fig. S3** PXRD patterns of  $\text{Ni(OH)}_2/r=2$  (red line) and  $\text{Ni(OH)}_2/r=10$  (black line) microspheres.

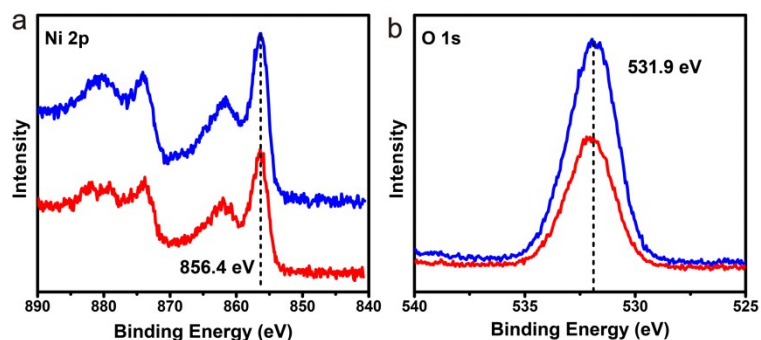


**Fig. S4** XPS of Ni(OH)<sub>2</sub>/r=0.5 (blue line) and Ni(OH)<sub>2</sub>/r=2 (red line) microspheres.

It was found that petal-like crystal Ni(OH)<sub>2</sub> aggregates were obtained without the introduction of AA into the system (Fig. S5b).

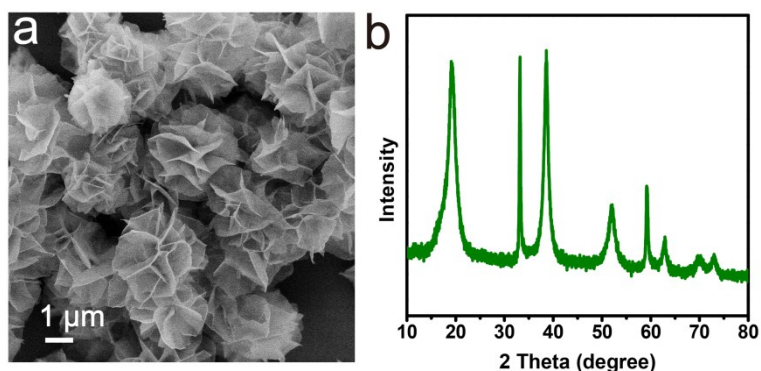


**Fig. S5** (a) SEM image and (b) PXRD pattern of the crystal Ni(OH)<sub>2</sub> aggregates synthesized without AA.

To further validate the role of the ligand in the metal-coordinating ligand self-assembly process, ultraviolet-visible spectra were used to monitor the reaction *in situ*. As observed in Fig. S6, an ascorbic acid (AA) aqueous solution presents a broad adsorption band in the region of 235–300 nm. The adsorption intensity decreases gradually as the reaction progresses, because more AA in the solution is employed to chelate with nickel species and interact with the surfactants.

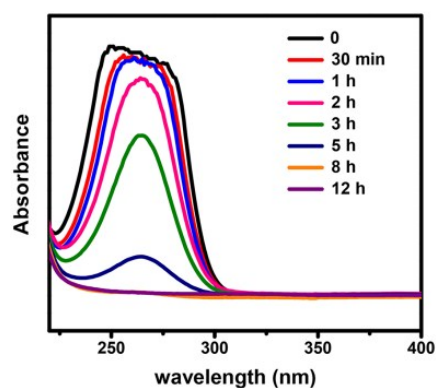


**Fig. S6** Ultraviolet-visible spectra of AA left in the reaction solution along with the reaction proceeding.

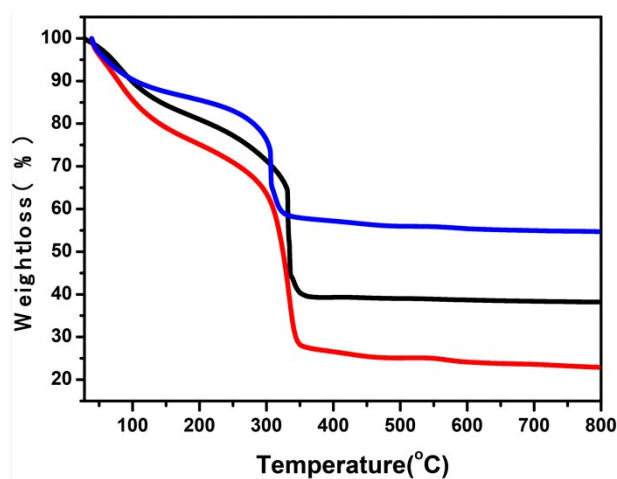


**Fig. S7** TG curves of the synthesized hierarchical  $\text{Ni}(\text{OH})_2$  microspheres:  $\text{Ni}(\text{OH})_2/r=0.5$  (black line),  $\text{Ni}(\text{OH})_2/r=2$  (red line), hollow  $\text{Ni}(\text{OH})_2/r=0.5$  (blue line).

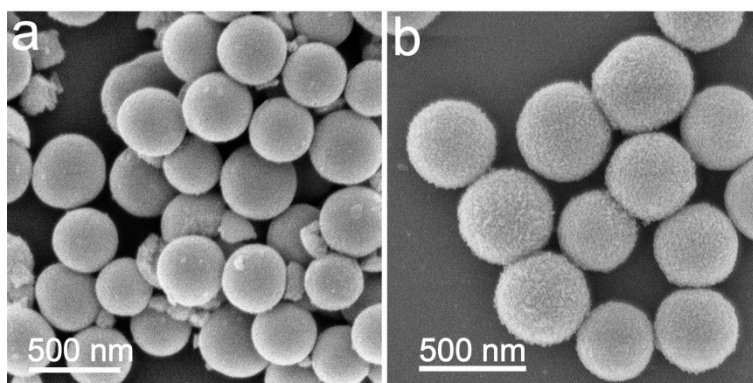


**Fig. S8** SEM images of calcined  $\text{NiO}$  microspheres: (a)  $\text{NiO}_{r=0.5-300^\circ\text{C}}$ ; (b)  $\text{NiO}_{r=2-300^\circ\text{C}}$ .

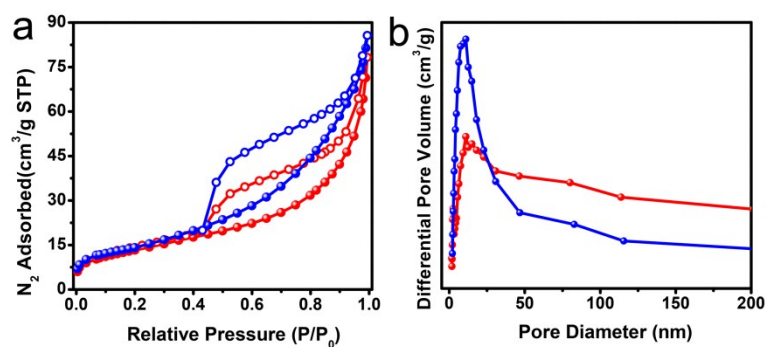


**Fig. S9** (a)  $\text{N}_2$  adsorption/desorption isotherms and, (b) the corresponding pore size distribution curves of the core-shell structured  $\text{Ni}(\text{OH})_2/r=2$  (red line) and  $\text{Ni}(\text{OH})_2/r=10$  (blue line) microspheres.

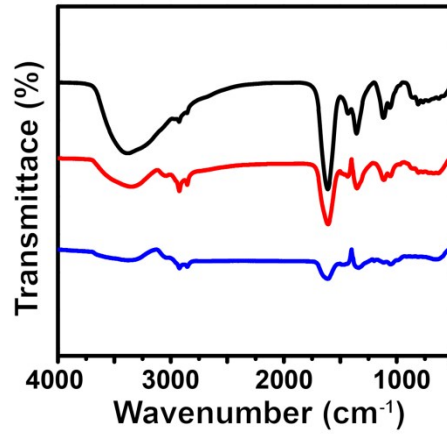


**Fig. S10** FTIR spectra of hierarchical Ni(OH)<sub>2</sub> microspheres: Ni(OH)<sub>2</sub>/r=0.5 (black line), Ni(OH)<sub>2</sub>/r=2 (red line), hollow Ni(OH)<sub>2</sub>/r=0.5 (blue line).

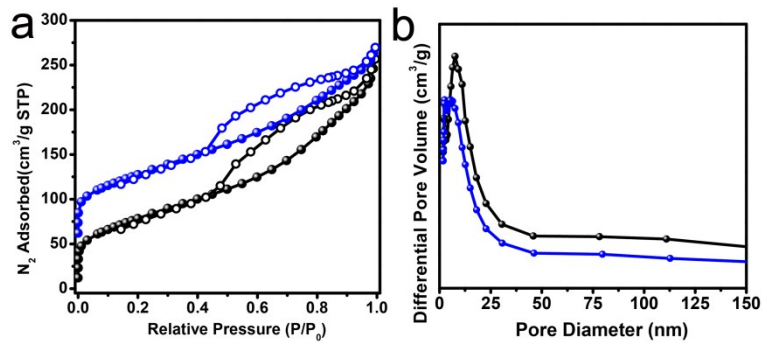


**Fig. S11** (a) N<sub>2</sub> adsorption/desorption isotherms and, (b) the corresponding pore size distributions curve and pore size distribution curves of the as-prepared NiO hierarchical mesoporous microspheres: NiO-300/r=5 (black line), NiO-300/r=10 (blue line). The N<sub>2</sub> adsorption/desorption isotherm is offset vertically by 50 cm<sup>3</sup> g<sup>-1</sup> for NiO-300/r=10.

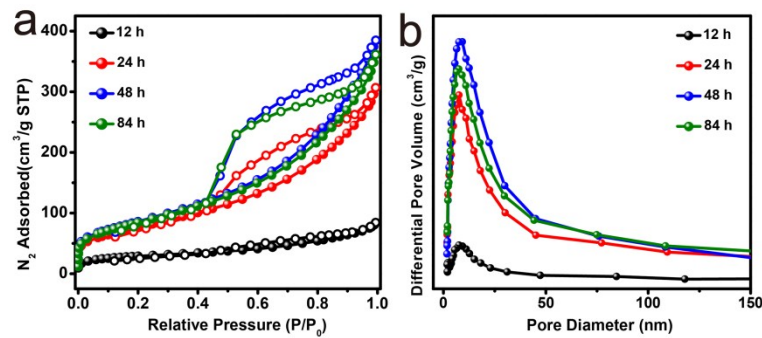


**Fig. S12** (a) N<sub>2</sub> adsorption/desorption isotherms and (b) the corresponding pore size distribution curves of the hollow mesoporous NiO microspheres with the reaction for different hours.

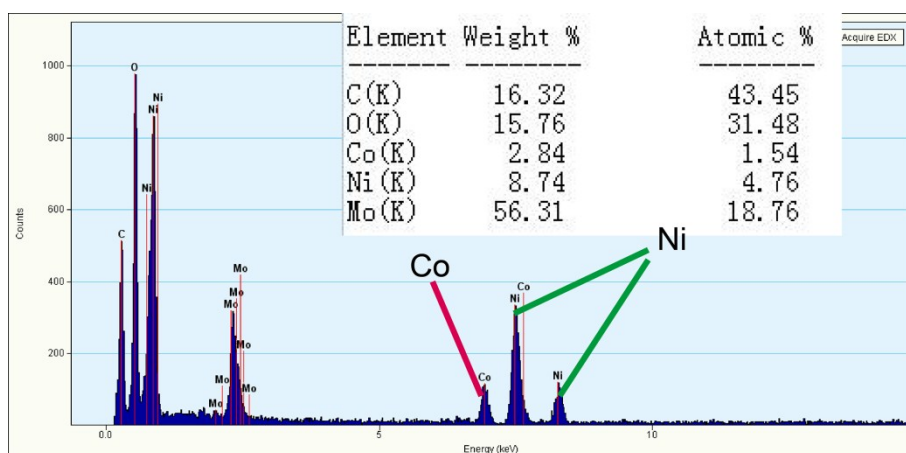


Fig. S13 Energy dispersive x-Ray spectroscopy (EDS) of the CoNiO<sub>x</sub> microspheres.

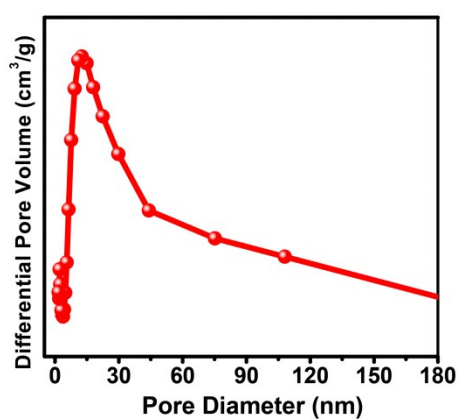


Fig. S14 Pore size distribution curve of Co<sub>0.32</sub>Ni oxide.

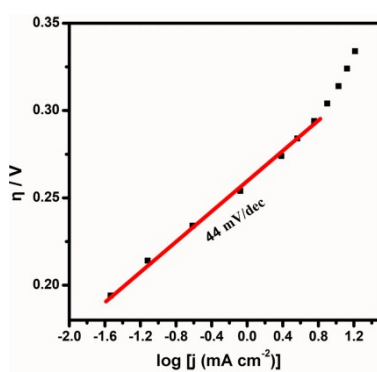
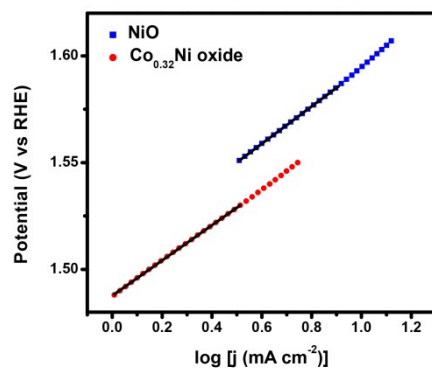
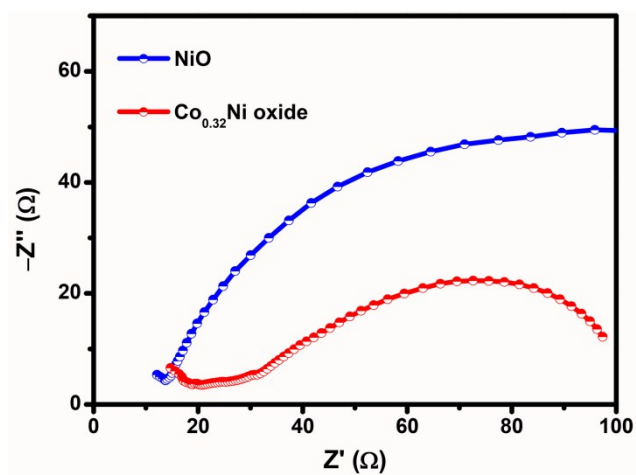


Fig. S15 Tafel plot of IrO<sub>2</sub>.



**Fig. S16** Tafel plots of hierarchical mesoporous NiO and Co<sub>0.32</sub>Ni oxide microspheres.



**Fig. S17** Electrochemical impedance spectroscopy (EIS) of the synthesized NiO and Co<sub>0.32</sub>Ni oxide catalysts.

**Table S1** comparison of electrochemical activity of hierarchical NiO<sub>r=2</sub>-300°C and Co<sub>0.32</sub>Ni oxide microspheres with other reported electrocatalysts for OER

| Ni-based material   | $\eta@10 \text{ mA cm}^{-2}$ (mV) | Tafel slope (mV dec <sup>-1</sup> ) | Reference   |
|---|-----------------------------------|-------------------------------------|---|
| NiS <sub>1.03</sub> -NSCs   | 270                               | 69                                  | <i>Small</i> , 2017, 1703273                                    |
| Fe-doped NiOx nanotubes   | 310                               | 49                                  | <i>Nano energy</i> , 2017, <b>38</b> , 167-174                  |
| Ni <sub>0.88</sub> Co <sub>1.22</sub> Se <sub>4</sub> hollow microparticles | 320                               | 58                                  | <i>Chem. Mater.</i> , 2017, <b>29</b> , 7032–7041               |
| $\alpha$ -Ni(OH) <sub>2</sub> /GC   | 330                               | 42                                  | <i>Adv. Energy Mater.</i> , 2016, 1502313                       |
| Ni <sub>x</sub> Co <sub>3-x</sub> O <sub>4</sub> nanowires                  | 337                               | 75                                  | <i>ACS Appl. Mater. Interfaces</i> , 2016, <b>8</b> , 3208-3214 |
| NiCoP/C nanoboxes   | 330                               | 96                                  | <i>Angew. Chem. Int. Ed.</i> 2017, <b>56</b> , 3897-3900        |
| Co <sub>0.32</sub> Ni oxide   | 340                               | 82                                  | <b>This work</b>  |
| NiO <sub>r=2</sub> -300°C   | 360                               | 87                                  | <b>This work</b>  |
| NiCo-POM/Ni   | 360                               | 126                                 | <i>Angew. Chem. Int. Ed.</i> <b>2017</b> , 56, 4941-4944        |
| NGO/Ni7S6   | 380                               | 45                                  | <i>Adv. Funct. Mater.</i> , 2017, 1700451                       |
| NiO@NF-6  | 405                               | 109                                 | <i>Nanoscale</i> , 2017, <b>9</b> , 4409-4418                   |
| NiCo <sub>2</sub> O <sub>4</sub>  | 540                               | 90                                  | <i>J. Mater. Chem. A</i> , 2014, <b>2</b> , 20823–20831         |